Liver Shape Analysis using Statistical Parametric Maps at Population Scale

Marjola Thanaj[1], Nicolas Basty[1], Madeleine Cule[2], Elena P Sorokin[2], Brandon Whitcher[1], Jimmy D Bell[1], E Louise Thomas[1]

1 Research Centre for Optimal Health, School of Life Sciences, University of Westminster, London, United Kingdom,

2 Calico Life Sciences LLC, South San Francisco, CA, United States

Corresponding Author: *m.thanaj@westminster.ac.uk*

Abstract

Background: Morphometric image analysis enables the quantification of differences in the shape and size of organs between individuals.

Methods: Here we have applied morphometric methods to the study of the liver by constructing surface meshes from liver segmentations from abdominal MRI images in 33,434 participants in the UK Biobank. Based on these three-dimensional mesh vertices, we evaluated local shape variations and modelled their association with anthropometric, phenotypic and clinical conditions, including liver disease and type-2 diabetes.

Results: We found that age, body mass index, hepatic fat and iron content, as well as, health traits were significantly associated with regional liver shape and size. Interaction models in groups with specific clinical conditions showed that the presence of type-2 diabetes accelerates age-related changes in the liver, while presence of liver fat further increased shape variations in both type-2 diabetes and liver disease.

Conclusions: The results suggest that this novel approach may greatly benefit studies aiming at better categorisation of pathologies associated with acute and chronic clinical conditions.

Key Words: Magnetic Resonance Imaging, Liver Volume, Surface mesh, Image Analysis, 3D mesh-derived phenotype, Statistical Parametric Maps, Type-2 Diabetes.

Abbreviations: T2D: Type 2 Diabetes; BMI: Body mass index; WHR: waist-to-hip ratio; AST:ALT: ratio of aspartate aminotransferase to alanine aminotransferase; FIB-4: Fibrosis-4 index; Liver PDFF: Liver percentage density fat fraction; MUR : Mass univariate regression; TFCE: Threshold-free cluster enhancement; SPMs: Statistical parametric maps; S2S: Surface-to-surface.

Introduction

Despite improvements in global health [1], incidence of liver disease continues to rise, with deaths due to hepatic conditions increasing by 400% since the 1970s (British Liver Trust - https://britishlivertrust.org.uk/), making it the leading cause of death in those aged 35-49 years in the UK (ONS 2019 - https://www.ons.gov.uk/). Significant progress has been made in recent years in the use of non-invasive imaging methods to measure the pathological changes that are features of increasingly common liver conditions. This includes non-alcoholic fatty liver disease (NAFLD) [2, 3], fibro-inflammation [4, 5] and fibrosis [6]. The prevalence of these conditions, associated with obesity, insulin resistance and type-2 diabetes (T2D), are likely only to increase further given the current obesogenic environment. New approaches are needed to differentiate between those with mild disease, compared with those at risk of more significant conditions (cirrhosis/end stage liver disease), and particularly those who may experience accelerated disease processes [7]. One potential approach to address these issues is the implementation of novel morphometric methods to

gain a deeper understanding of the processes underpinning the development and progression of many clinical conditions [8]. For instance, investigating whether changes beyond simple volume or fat measurements, such as liver shape, are associated with particular environmental risk factors, or whether they can be differentially related to the aetiology of a particular condition. These methods may potentially provide insight into different mechanisms of disease development and enable optimised treatment strategies to be developed.

Automated segmentation of the liver to produce image-derived phenotypes (IDPs) such as volume or fat deposition measurements are becoming more commonplace at scale as deep learning methods gain traction [9]. While these methods enhance our understanding of the liver at a population level, they are limited when it comes to providing additional knowledge regarding morphological, functional and regional variation in response to a particular condition.

Mapping organ segmentations to a standardised three-dimensional (3D) surface mesh, enables many thousands of measurements relating to variation in organ shape to be performed using statistical parametric maps (SPMs). A similar widely applied technique, which transforms the 3D surface mesh measurements into a smaller number of principal components, known as shape parameters, has been used to characterise variations in organ shape across a population. These approaches have been successfully applied in neuroimaging [10, 11], abdominal computer tomography (CT) images [12, 13], and cardiac imaging [14, 15] and they have shown to be useful in identifying genetic interactions with cardiac pathology [16] and brain ageing [17]. However, they have been less frequently applied to abdominal organs, where morphological changes are known to take place in a variety of clinical conditions [18, 19].

In the current study we have applied SPM methods to determine morphological variations in the liver and their potential association with anthropometric traits and clinical conditions.

Methods

Data

The UK Biobank [20] is a population-based study in which 500,000 participants aged 40 to 70 years were recruited for deep phenotypic profiling. There is also a currently ongoing imaging sub-study, in which 100,000 of the participants have been recruited to undergo an imaging protocol including MRI of the brain, the heart, and the abdominal region. The abdominal scans include a neck-to-knee Dixon 3D acquisition that can be used to derive volumes of adipose tissue, skeletal muscle and abdominal organs. Full details regarding the UK Biobank abdominal acquisition protocol have previously been reported [21]. We processed and segmented the data using our automated methods [9]. In this study on liver morphology, we included 41,800 participants with Dixon MRI data acquired at the imaging visit, between 2014 and 2020 with data comprising imaging, health-related diagnoses and biological measurements.

Participants with missing clinical, anthropometric or biochemical data, as well as those with Dixon MRI datasets that did not have full anatomical coverage were excluded from the study. We then performed quality control by visually inspecting potential outliers in the 3D liver mesh-derived phenotype (i.e. extremely high values). Overall, from the initial 41,800 participants, 33,434 participants were included in the final analysis (20% of data excluded).

Fully anonymized participant data was obtained through UK Biobank Access Application number 44584. The UK Biobank has approval from the North West Multi-Centre

Research Ethics Committee (REC reference: 11/NW/0382) written informed consent was obtained from all participants prior to inclusion in the UK Biobank.

Phenotype Definitions

Anthropometric measurements including age, body mass index (BMI), waist and hip circumferences were taken at the UK Biobank imaging visit and ethnicity was defined based on the continental genetic ancestry (https://pan.ukbb.broadinstitute.org). AST:ALT ratio, defined as the ratio of aspartate aminotransferase (AST) to alanine aminotransferase (ALT), commonly used to indicate presence of more advanced liver disease including fibrosis and cirrhosis [22, 23] was calculated from the biological samples taken at the initial assessment visit. The fibrosis-4 index (FIB-4), also designed to identify more advanced stages of liver disease and fibrosis in particular, was calculated as previously described [24] using age, AST, ALT and platelet count taken from the initial assessment visit. Diagnosis of liver disease and T2D was obtained from UK Biobank hospital records and self-reported information (see Disease Categories in supporting information). Due to the relatively limited number of scanned participants within the UKBB diagnosed with specific liver diseases, a broad umbrella definition of liver disease was implemented which included, alcoholic liver disease, fibrosis, cirrhosis, and chronic hepatitis.

Study Design

Template Definition

Deformation of an image to a standard organ template is a key part of MRI organ shape assessment. Given the potential variation in morphology, it is important to identify a suitable population sample size for constructing a template image [25]. To assess the impact of population size on template construction, we constructed three distinct templates using liver segmentations from a gender-balanced European ancestry cohort of 20, 100 and 200 participants with BMI<25 kg/m^2 and low liver fat (<5%). The characteristics for each template population are provided in S1 Table. To test the 3 templates, we selected 500 participants,

derived from the full cohort, with European genetic ancestry, aged between 46 and 62 years old, without any disease reported or diagnosed here [26] (S2 Table). We then registered the three liver templates to the 500-participant cohort and investigated the associations between the 3D mesh-derived phenotype and the anthropometric covariates across the three templates.

Association between mesh-derived phenotypes, IDPs and Disease

To assess the associations between the 3D mesh-derived phenotype, the anthropometric covariates and liver IDPs (volume, fat, iron), we first analysed the liver MRI data from the entire UK Biobank imaging cohort. The cohort of 33,434 participants was 97.6% European, 48.7% male and aged between 44 and 82 years old (S3 Table). To determine the potential association between disease and liver shape, we first selected diseases that are known from previous studies to impact liver health, and are associated with changes in liver fat accumulation or volume [9]. These included 449 participants with liver disease (207F/242M; 48-81 years old; BMI 18.6-43.8 kg/m²) and 1,780 participants with T2D (67% males; 46-82 years old; BMI 18.3-50.1 kg/m²) (S4 Table).

Image Registration and Mesh Construction

The process for template construction of the liver has been previously described [27]. Here, we constructed three distinct templates using liver segmentations from 20, 100 and 200 subject-specific volumes in order to evaluate the impact of cohort size on template construction. It also allows us to test if cohort size influenced the statistical associations in our mesh-based analysis. We constructed surface meshes from each template using the marching cubes algorithm and smoothed using a Laplacian filter [28]. The template construction was performed using ANTs software (https://picsl.upenn.edu/software/ants) with mutual information as the similarity metric, the B-spline non-rigid transformation model and default parameters otherwise.

Surface meshes were first constructed from each subject's segmentations using marching cubes algorithm and smoothed using a Laplacian filter. Rigid registration was then used to remove the position and orientation difference between all subject-specific surfaces and template surfaces and an affine transformation with nearest neighbour interpolation was computed between template and subject segmentations. The resulting affine transformations were used to warp the template to the subject's space. The template segmentation is then mapped into each subject segmentation by computing a non-rigid transformation modelled by a free-form deformation, based on B-Splines, with label consistency as the similarity metric between the subject and template liver segmentations [29]. To enable subject comparison with vertex-to-vertex correspondence, the template mesh is then warped to each subject mesh using the deformation fields obtained from the non-rigid registration. Hence, all surface meshes are parameterised with the same number of vertices (approximately 18,000). This ensures each vertex is anatomically accurate and consistent across all subjects while preserving the size and shape information for subsequent analysis [28].

To determine the regional outward or inward adaptations in the liver surface in comparison to an average liver shape, the surface-to-surface (S2S) distance, a 3D mesh-derived phenotype for each subject was measured. This was achieved by computing the signed distance between each vertex in the template mesh and each corresponding vertex in the subjects' mesh. This indicates positive distances for outward expansion in the subject's vertices compared to template vertices and negative distances for inward shrinkage in the subject's vertices. Finally, after performing the aforementioned manual quality control on the S2S values, all values were between -48.3 to 70.5 mm. All the steps above were performed using the Image Registration Toolkit (IRTK) (https://biomedia.doc.ic.ac.uk/software/irtk).

Mass Univariate Regression

Associations between the S2S values and anthropometric variables were modelled using a linear regression framework. We applied threshold-free cluster enhancement (TFCE) [30] and permutation testing to assess the associations between S2S distances and anthropometric covariates, as well as liver fat and iron content. These were adjusted for relevant covariates with correction to control the false discovery rate (FDR), as previously described [27]. Specifically, we performed mass univariate regression (MUR) analysis using a refined version of the R package *mutools 3D [31]* and adjusted for multiple comparisons by applying the FDR procedure [32] to all the TFCE p-values derived from each vertex and each model using 1,000 permutations. The estimated regression coefficients $\hat{\beta}$ for each of the relevant covariates and their related p-values were then displayed at each vertex in the mesh on the whole 3D liver anatomy, providing the spatially-distributed associations. The MUR model for deriving associations between clinical parameters and a 3D phenotype is outlined in Supplementary Fig. S1.

To determine which factors influence the design and performance of the liver template, we used a regression model to address: (1) how many participants are required to construct a representative liver template, (2) whether the template population size affected the associations between the S2S and the anthropometric covariates, (3) which factors have an impact on regional S2S distances and (4) how are the changes in S2S distances linked to liver disease and T2D.

We constructed three models adjusting for additional covariates. **Model 1** was adjusted for age, gender, ethnicity, body mass index (BMI) and waist-to-hip ratio (WHR), liver fat (referred to as proton density fat fraction (PDFF)) and liver iron concentration with correction to control the FDR. To investigate the morphological changes related to liver function **Model 2** had all the covariates from model 1 plus AST:ALT, FIB-4 index and disease conditions. We further adjusted with interaction terms between age and disease status and between liver fat and disease. In order to test whether there is a circadian effect

in the liver morphology, **Model 3** included all the covariates from model 2 plus time of the day for the MRI scan, discretised into hours of the day.

Results

Template Consistency

We constructed 3 separate template meshes using gender-balanced cohorts of 20, 100 and 200 participants and computed the distances between each template mesh for each subpopulation (Supplementary Fig. S2). The results showed that cohort size had little impact on the shape of the template, with differences less than 8mm, especially for the templates constructed using 100 participants compared with the 200-participant template.

We then investigated for each template the associations between S2S distances and anthropometric variables, adjusting for the covariates in Model 1. Here we only looked at the associations between BMI and WHR with S2S distances, as only these variables showed statistically significant associations. The 3D SPMs, with the TFCE corrected p-values, between BMI and S2S distance on the previously selected 500-participants cohort showed that the distribution of the corrected p-values were consistent across all three different templates (Supplementary Fig. S3). As shown in Table 1, there was no apparent difference in the areas of association between BMI and WHR with S2S distances across the three templates.

Significance area	**20-participant template**		**100-participant template**		**200-participant template**	
	BMI	**WHR**	**BMI**	**WHR**	**BMI**	**WHR**

Total	58.08%	14.48%	55.20%	18.28%	56.73%	12.12%
$\hat{\beta} < 0$	2.74%	4.79%	3.28%	7.42%	2.66%	4.67%
$\hat{\beta} > 0$	55.34%	9.69%	51.92%	10.85%	54.07%	7.46%

Table 1. Significance areas from the association between BMI and WHR with S2S distances on a 500-participants cohort, in the MUR model using a template with 20, 100 and 200 participants. The significance area is the percentage of vertices on the liver mesh where the regression coefficients are statistically significant ($p < 0.05$) after adjustment for multiple comparisons. The total area has been split into areas of negative ($\hat{\beta} < 0$) and positive ($\hat{\beta} > 0$) associations.

In order to test template consistency on a disease population, all three templates were registered on a cohort of 449 participants with liver disease and the 3D S2S phenotype computed between template and participants' surface. We then modelled the associations between the S2S distances and anthropometric variables adjusting for the covariates in model 1. The TFCE corrected p-value maps on the cohort with liver disease were consistent across the three templates, with little difference in the significance area for the association between BMI and S2S distances (97.58% using the 20-participant template, 97.46% using the 100-participant template and 96.43% using the 200-participant template) (S4 Fig and Table 2).

Significance area	**20-participant template**		**100-participant template**		**200-participant template**	
	BMI	**WHR**	**BMI**	**WHR**	**BMI**	**WHR**

Total	97.58%	91.02%	97.46%	90.31%	96.43%	90.98%
$\hat{\beta} < 0$	0.01%	0.01%	0%	0%	0%	0%
$\hat{\beta} > 0$	97.57%	91.01%	97.46%	90.31%	96.43%	90.98%

Table 2. Significance areas from the association between BMI and WHR with S2S distances on a cohort with liver disease (N=449), in the MUR model using a template with 20, 100 and 200 participants. The significance area is the percentage of vertices on the liver mesh where the regression coefficients are statistically significant ($p < 0.05$) after adjustment for multiple comparisons. The total area has been split into areas of negative ($\hat{\beta} < 0$) and positive ($\hat{\beta} > 0$) associations.

Associations with Anthropometric Characteristics, Liver IDPs and Disease

As the liver template was relatively insensitive to the number of participants included, we performed all subsequent analyses using the 200-participant template. We proceeded to register the template on the full cohort (N=33,434), computing S2S distances between the template and surface of each individual liver mesh and performed MUR analysis adjusting for the covariates in Model 2.

A summary of the model for the whole cohort, representing the regression coefficients and the significance areas on the liver, is provided in Table 3 and Supplementary Fig. S5. The SPMs that represent associations between S2S distances and the anthropometric measurements and liver IDPs with units in standard deviations for each covariate, are shown in Fig. 1.

Lower S2S distances were associated with greater age over 96.63% of the liver, with a median change of -0.11 mm/year, while BMI and WHR had statistically significant positive associations with S2S distances, covering 97.82% and 58.11% of the liver, respectively. The

AST:ALT ratio showed mostly statistically significant positive association with S2S distances in the anterior part of the left lobe and the posterior part of the right lobe, with a median difference of 0.30 mm (significance area = 48.05%). FIB-4 index on the other hand showed a median S2S distance of -0.22 mm (significance area = 82.62%). Liver PDFF was positively associated with S2S distances, showing median outward shape variations of 0.26 mm/%, whereas liver iron concentration was associated with S2S distances of -0.59 mm/(mg/g) in the anterior part of the right lobe and the posterior part of the left lobe and a median 0.34 mm/(mg/g) in the anterior part of the left and caudate lobe. Additionally, we included MRI scan time as an additional covariate in the model since liver size is known to vary during the day [9], but this had no apparent effect on any of the associations (Supplementary Table S5, Supplementary Fig. S6).

A diagnosis of liver disease was associated with a median S2S of -2.13 mm when compared to the controls (significance area = 21.90%) in the anterior part of the right lobe as well as at the posterior part of left and right lobe and a median of 1.95 mm (significance area = 25.14%) in the anterior part of the left lobe. T2D was positively associated with S2S distances, with a median of 2.42 mm for participants with T2D covering a significance area of 86.40% of the liver. The time of day at which the MRI scan was conducted had no effect on the associations between S2S and T2D, although we observed a reduction in the significance area for the associations between S2S and liver disease (significance area = 28.34%, Supplementary Table S5, Supplementary Fig. S6).

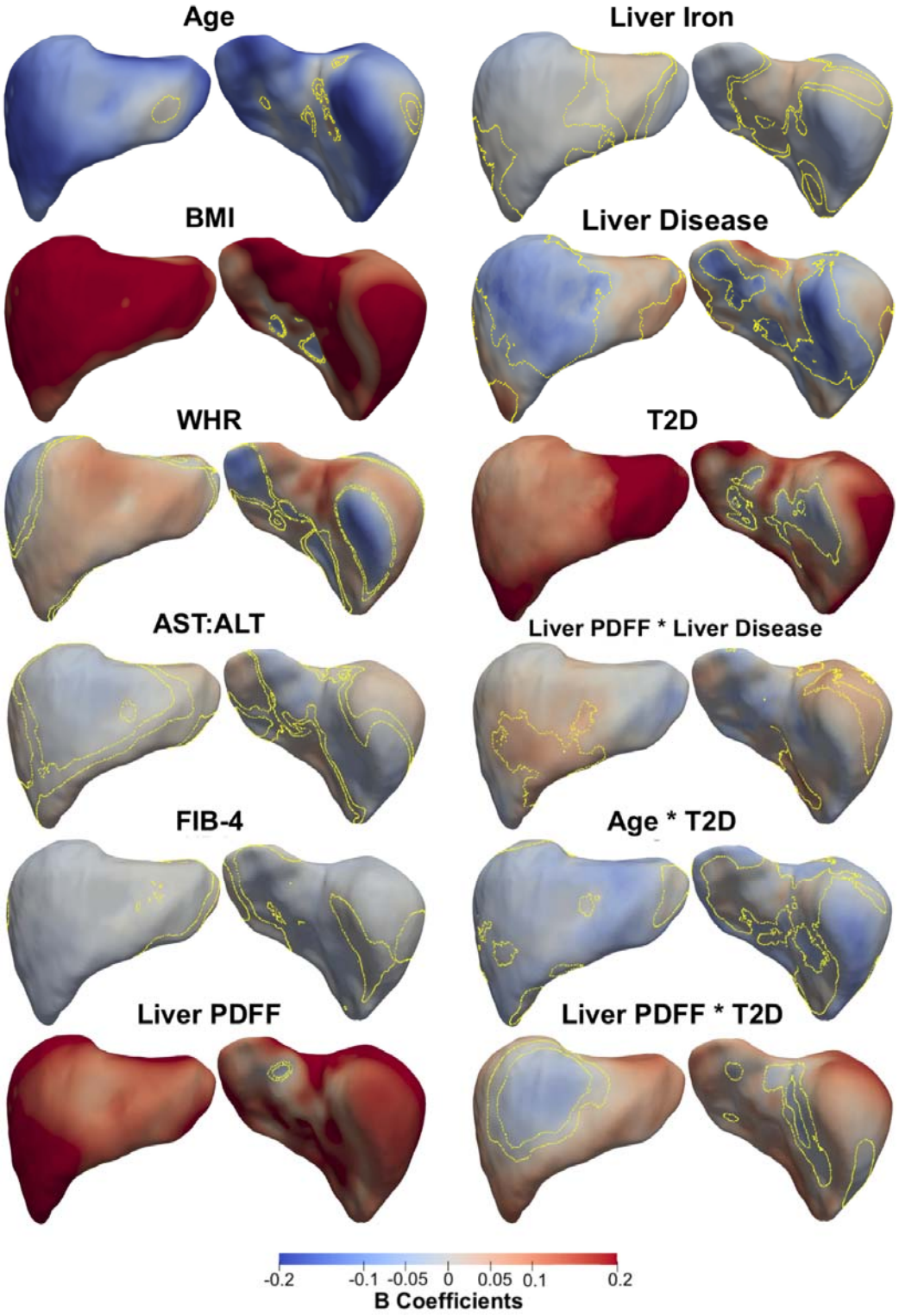

Figure 1. Three-dimensional statistical parametric maps (SPMs) of liver morphology, two projections are shown for each SPM providing anterior (left) and posterior (right) views of the liver. The SPMs show the local strength of association for each covariate in model 2 with

S2S distances on the full cohort (N=33,434). Yellow contour lines indicate the boundary between statistically significant regions ($p < 0.05$) after correction for multiple testing, with positive associations in red and negative associations in blue. Standardised regression coefficients are shown with units in standard deviations for each covariate. BMI: body mass index, WHR: waist-to-hip ratio, AST:ALT: aspartate aminotransferase/alanine aminotransferase ratio, FIB-4: Fibrosis-4 score, Liver PDFF: Liver percentage density fat fraction, T2D: type-2 diabetes.

	$\hat{\beta} < 0$		$\hat{\beta} > 0$		**Total**
	Beta coefficients	Significance area	Beta coefficients	Significance area	Significance area
Age ($yrs.$)	-0.11 (0.06)	96.63%	0.02 (0.04)	1.46%	98.10%
BMI (kg/m^2)	-0.08 (0.07)	1.61%	0.30 (0.22)	97.82%	99.43%
WHR	-3.88 (4.02)	33.99%	3.87 (3.65)	58.11%	92.10%
AST:ALT	-0.32 (0.32)	35.17%	0.30 (0.29)	48.05%	83.22%
FIB-4	-0.22 (0.17)	82.62%	0.23 (0.13)	2.09%	84.70%
Liver PDFF (%)	-0.03 (0.02)	0.17%	0.26 (0.10)	99.65%	99.82%
Liver Iron (mg/g)	-0.59 (0.74)	58.00%	0.34 (0.32)	24.99%	82.98%
Liver disease	-2.13 (2.95)	21.90%	1.95 (2.43)	25.14%	47.05%
T2D	-0.61 (0.77)	5.35%	2.42 (1.94)	86.40%	91.76%

Age * Liver disease	ns	ns	ns	ns	ns
Liver PDFF * Liver disease	-0.09 (0.01)	0.09%	0.09 (0.03)	12.59%	12.68%
Age * T2D	-0.03 (0.02)	71.23%	0	0%	71.23%
Liver PDFF * T2D	-0.06 (0.04)	6.24%	0.10 (0.08)	82.84%	89.08%

Table 3. Significance areas for covariates in the MUR model between the anthropometric covariates and liver IDPs (N=33,434) in model 2. The total area has been split into areas of positive and negative associations. The regression coefficients are presented as median (interquartile range - IQR) and the significance areas as a percentage (%) of the vertices. Where BMI: body mass index, WHR: waist-to-hip ratio, AST:ALT: aspartate aminotransferase/alanine aminotransferase ratio, FIB-4: Fibrosis-4 score, Liver PDFF: Liver percentage density fat fraction, T2D: type-2 diabetes, ns: not significant.

We undertook further analysis to determine whether there was an interaction between clinicalstate and factors such as age and liver PDFF adjusted for all covariates in Model 2. Our results varied according to the disease of interest. While there were no significant associations for the interaction between age and liver clinical condition, we found a median association of -0.14mm/year in T2D participants, compared with -0.11mm/year in non-T2D participants, over a similar anatomical region. The interaction term between age and T2D in this model was significantly different from zero, with a significance area = 71.23% (Table 3 and Fig. 1). The association between age and S2S distances in participants with and without T2D are directly compared in Fig. 2, where participants diagnosed with T2D display accelerated decreases in the anterior part of the left and right lobe as well as at the posterior part of left and right lobe of the liver.

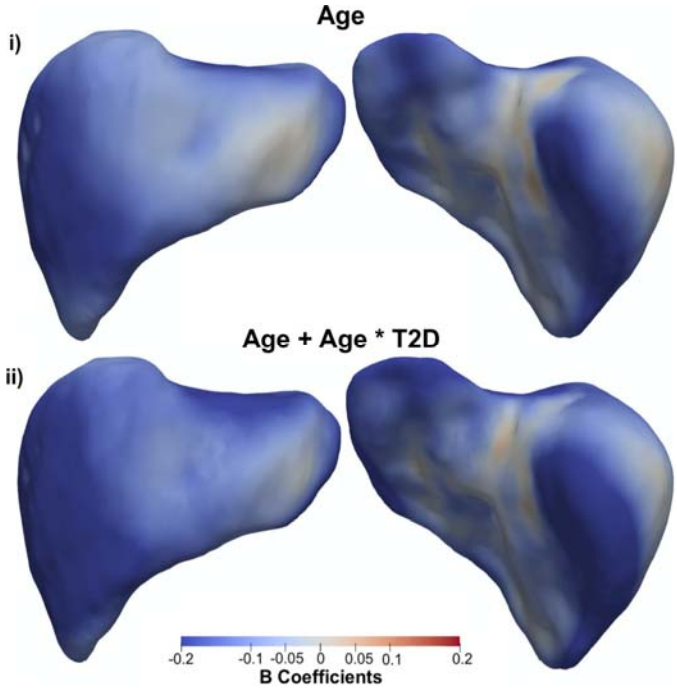

Figure 2. Three-dimensional statistical parametric maps (SPMs) of liver morphology, projections are anterior (left) and posterior (right). The SPMs show the local rate of change as a function of age for S2S distances in participants (i) without T2D versus those (ii) with T2D on the full cohort (N=33,434). Positive associations are in red and negative associations in blue. Standardised regression coefficients are shown with units in standard deviations.

The presence of liver PDFF in participants with liver disease resulted in an additional median variation of 0.09 mm/% over an area 12.59% of the liver, in addition to the median variation of 0.26 mm/% associated with the main effect of liver PDFF (Table 3 and Fig. 1). Interestingly this effect was no longer significant after including scan-time as an additional covariate in the model (Supplementary Table S5, Supplementary Fig. S6). A change of similar magnitude, over a much larger proportion of the liver was observed for the interaction between liver PDFF and T2D (Table 3 and Fig. 1). Here we observed an accelerated increase in S2S distances with a median change of 0.10 mm/%, over the majority of the liver surface area (significance area = 82.84%), in addition to the median increase of 0.26 mm/%

for the main effect of liver PDFF. The rates of change in S2S distances due to changes in liver PDFF for participants with liver disease only, with T2D only and those without either disease are directly compared in Fig. 3. The local variations associated with liver PDFF fluctuates significantly with disease diagnosis. Participants diagnosed with liver disease (Fig. 3ii) display accelerated increases in S2S distances in the anterior and posterior parts of the right lobe with increasing liver PDFF, with slight decreases in the rate of change in both the anterior and posterior left lobe when compared to participants without either liver disease or T2D. Participants with T2D (Fig. 3iii) display accelerated increases in S2S distances in the anterior and posterior right lobe and the posterior left lobe when compared to participants without T2D, and display substantial decreases in the rate of change in S2S distances in the anterior left lobe when compared to participants who have been diagnosed with liver disease but not T2D or participants who have not been diagnosed with either liver disease or T2D.

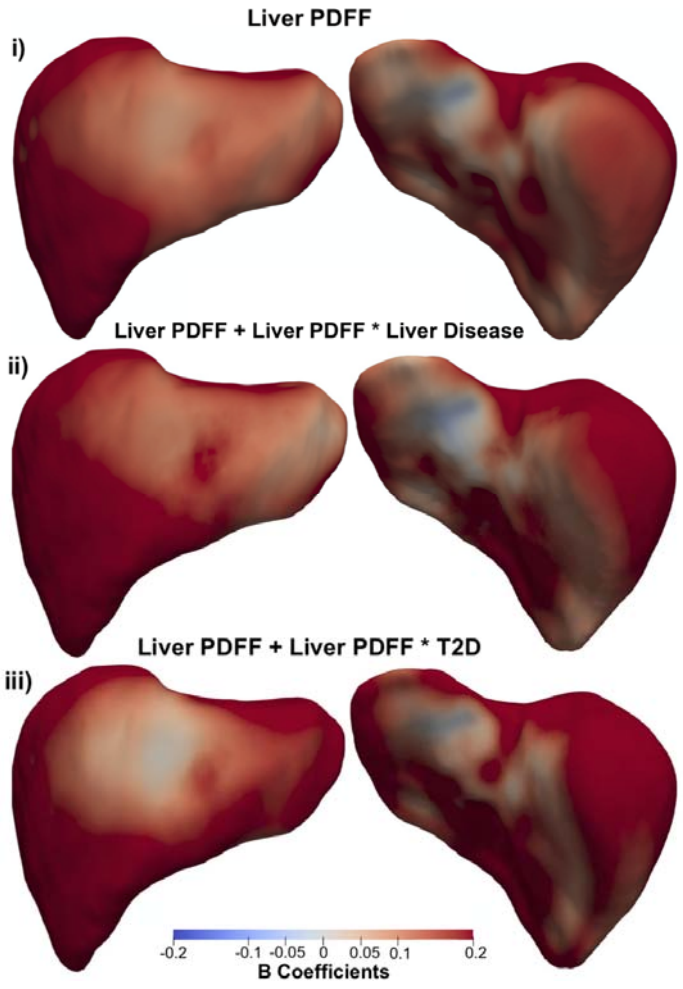

Figure 3. Three-dimensional statistical parametric maps (SPMs) of liver morphology, projections are anterior (left) and posterior (right). The SPMs show the rate of change as a function of liver PDFF for S2S distances in participants (i) without liver disease or T2D, (ii) with liver disease only and (iii) with T2D only on the full cohort (N=33,434). Positive associations are in red and negative associations in blue. Standardised regression coefficients are shown with units in standard deviations.

Discussion

In this study, we mapped local shape variations across the liver and determined how these changes were associated with anthropometric, phenotypic and health traits. To achieve this we constructed surface meshes from liver segmentations of 33,434 participants from the UK Biobank. Previous studies using similar SPMs have suggested that this is a useful technique in neuroimaging [10] and cardiac imaging [14], enabling the associations between phenotypic and genetic variation in specific anatomical regions to be mapped [16].

First, we constructed a representative liver template, and showed that a 200-participant template was sufficient to represent the broader cohort. Indeed, the number of participants included in the template construction did not impact the power of the statistical analysis across a 500-participant test cohort, or a second cohort of 479 participants with liver disease. This is in line with previous studies that found a cohort with 100 participants was sufficient to construct a representative cardiac template to investigate the shape of the left ventricle [28].

Liver size has been explored extensively using a variety of approaches from autopsy measurements [33], CT [34], ultrasound [35], and MRI [19], as well as regression-based algorithms designed to predict liver size based on body surface area [36]. Given accurate assessment of liver volume is essential for many aspects of hepatic surgery and determining

391 disease progression [37], suitable methods are needed. However, until recently, the manual
392 annotation required to make true volumetric measurements of the liver from CT and MRI
393 images has been extremely time consuming. Imaging studies tended to rely on more easily
394 measured metrics, such as liver span or diameter [38, 39], or calculation of volume indices
395 from the measurement of multiple diameters [40]. Consequently, these approaches limit in
396 depth morphometric assessment and only provide information associated with overall
397 changes to liver size or volume. The SPM method implemented in the current study
398 demonstrates significant regional variations in liver shape associated with anthropometric
399 variables and disease status, including simultaneous inwards and outwards adaptations.
400 These novel phenotypic variables may be useful in longitudinal population studies, as well as
401 determining trajectories of progression in aggressive clinical conditions, including monitoring
402 liver cirrhosis and hepatic oncology. It may also be a powerful adjunct tool in clinical trials
403 aimed at reversing liver conditions such as cirrhosis.
404
405 While studies of liver volume have generally focussed on patient populations, there is
406 increasing interest in understanding how hepatic volume and form is influenced by age,
407 anthropometry and metabolic markers in the wider population [9, 40]. Despite this, few
408 studies employ methods that enable precise measurements of these parameters, particularly
409 with regard to regional variation in liver shape and size. In the present study we observed
410 that decline in the liver S2S distances were associated with increasing age. This is in
411 agreement with previous observations, by ourselves and others, that overall liver volume
412 decreases with age [9, 35, 41]. However, there are some ultrasound reports suggesting liver
413 size increases with age [38]. This discrepancy may relate to variations in methodology since
414 ultrasound measurements of liver diameter may not reflect overall changes in liver volume.
415 This clearly reinforces the importance of absolute volumetric measurements, which, when
416 combined with statistical parametric mapping, enables simultaneous extraction of global and
417 local changes.
418

We found a strong and distinct regionality in liver morphometry which was associated with anthropometric traits, liver PDFF and disease. Higher liver PDFF was significantly associated with positive S2S distances, suggesting that hepatic fat is associated with both liver size and shape, with some clear regional variations. We also found that higher BMI and WHR were strongly associated with positive S2S distance, in line with others who have reported a positive correlation between liver size and anthropometric variables [39, 40]. We also explored whether the time of day the participants were scanned was associated with S2S distances, given we have previously shown this to be associated with fluctuations in liver volume [9]. However, we did not find a measurable effect.

We also investigated whether conditions with known involvement of hepatic function had discernible effects on our S2S measurements. For this we selected T2D, commonly associated with increased deposition of liver PDFF, and subjects with known liver conditions, which we expected to be associated with a more adverse phenotype. We found that T2D was associated with outward shape variations in the liver after adjusting for PDFF, suggesting that T2D affects liver morphology. It is well recognised that T2D is associated with a range of liver conditions, with the prevalence of NAFLD in patients with T2D reported to be 55% and NASH 37.3% [42], substantially higher than the proportion of individuals in the general population with NAFLD (19.9%) [3] or NASH (2.2%) [43]. Given the clinical heterogeneity of our current T2D cohort, in terms of time of diagnosis and medication, as well as the possibility of collider bias or reverse confounding, it is impossible to identify causal mechanisms for the observed variation in S2S distances. Interestingly when we considered the interaction between age and disease, we found no statistically significant interaction for liver disease, but there was a significant interaction between age and the presence of T2D. We also considered whether the interaction between disease and the presence of liver PDFF was associated with S2S distances. Moreover, the variations covered a larger proportion of the liver in T2D compared with liver disease. This may suggest that the hepatic tissue in T2D retains its overall relative plasticity (i.e. less fibrotic-

447 cirrhotic tissue), while in liver disease there may be regions that have reduced capacity to
448 accumulate fat or lost their plasticity and thus be less responsive to geometrical changes.
449 Future work in patients with biopsy-characterised hepatic tissue should help to shed light on
450 the heterogeneity of response to the interaction between liver fat accumulation and liver
451 health status.
452
453 Our analyses allow for the visualisation of significant regional changes across the
454 liver. Of note, we found that diagnosis of liver disease was associated with an inward shape
455 variation at the anterior part of the right lobe, and posterior parts of the left and right lobes
456 accompanied by an outward increase in liver S2S distances in the anterior part of the left
457 lobe. Previous studies have suggested that statistical shape modelling may be used to
458 predict and stage fibrosis based on changes in liver shape [13, 44]. With limited outcome
459 and longitudinal data in the current study, the clinical significance of these changes,
460 particularly the simultaneous regional inward and outward deformations in S2S distances are
461 unclear. However, histological and radiological studies of the liver in patients with cirrhosis
462 have shown that the degree of volume reduction and fibrosis is greater in the right lobe
463 compared to the caudate lobe (which reportedly expands) [45]. This suggests regional
464 changes in S2S distances may reflect physiological processes in the liver. It is well
465 established that many diseases do not progress uniformly across the liver, with differences
466 reported within different zones (periportal, mid-lobular and pericentral) of the liver lobule,
467 which may reflect populations, different cell types, metabolic function and differences in
468 blood flow [46]. Whilst it is premature to adjudicate a mechanism responsible for the
469 changes described in the current study, the regional shape differences associated to both
470 AST:ALT and FIB-4, hinting at hepatocellular changes underpinning the variation in S2S
471 distances.
472
473 Our study was not without limitations. To ensure sufficient numbers of participants in
474 the liver disease group, we included all participants in the imaging cohort who had a

diagnosis of liver disease, regardless of aetiology (alcoholic, toxic and inflammatory liver disease, hepatitis, fibrosis and cirrhosis). This precludes us from a more in-depth granular analysis, although our data does suggest that hepatocellular damage, particularly in more advanced disease stages, resulted in significant S2S changes across the liver. Variation in disease aetiology, the point of disease progression and the impact of on-going treatment may further confound the interpretation of our observations in the liver disease cohort.

Conclusion

This study demonstrates that methods to assess changes in liver morphology, beyond simplistic volumetric analysis, can be applied at scale. In a population-based study we show that inter- and intra-subjects' morphometric variations are associated with age, body composition and liver phenotypes, as well as disease. The approach developed here will allow large-scale studies of patient-based cohorts, enable disease-specific changes in morphology to be defined and tracked during both progression and remission and facilitate disease prediction and stratification.

Declarations

Competing interests

M.C. and E.P.S. are employees of Calico Life Sciences LLC. M.T., N.B., B.W., J.D.B. and E.L.T. declare no competing interests.

Ethics approval and consent to participate

The data resources used in this study have approval from ethics committees. Full anonymised images and participants metadata from the UK Biobank cohort was obtained through UK Biobank Access Application number 44584. The UK Biobank has approval from the North West Multi-Centre Research Ethics Committee (REC reference:

11/NW/0382), and obtained written informed consent from all participants prior to the study. All methods were performed in accordance with the relevant guidelines and regulations as presented by the relevant authorities, including the Declaration of Helsinki https://www.ukbiobank.ac.uk/learn-more-about-uk-biobank/about-us/ethics .

Consent for publication

Not applicable.

Availability of data and materials

The data that support the findings of this study are available from the UK Biobank (https://www.ukbiobank.ac.uk), but restrictions apply to the availability of these data, which were used under license for the current study, and so are not publicly available. Data are however returned by us to the UK Biobank where they will be fully available on request.

Funding

This study was funded by Calico Life Sciences LLC.

Authors' contributions

J.D.B., E.L.T., M.T. and M.C. conceived the study. J.D.B., B.W., E.L.T., N.B. and M.T. designed the study. M.T., N.B., B.W., E.P.S. and M.C. implemented the methods and performed the data analysis. M.T. defined the disease and physiological condition categories. M.T. performed the image and statistical analysis. E.L.T., B.W., M.T., J.D.B., and N.B. drafted the manuscript. All authors read and approved the manuscript.

Acknowledgements

This research has been conducted using the UK Biobank Resource under Application Number 44584.

References

1. Vos et al. Global burden of 369 diseases and injuries in 204 countries and territories, 1990-2019: a systematic analysis for the Global Burden of Disease Study 2019. Lancet. 2020;396:1204–22.

2. Szczepaniak LS, Nurenberg P, Leonard D, Browning JD, Reingold JS, Grundy S, et al. Magnetic resonance spectroscopy to measure hepatic triglyceride content: prevalence of hepatic steatosis in the general population. Am J Physiol Endocrinol Metab. 2005;288:E462–8.

3. Wilman HR, Kelly M, Garratt S, Matthews PM, Milanesi M, Herlihy A, et al. Characterisation of liver fat in the UK Biobank cohort. PLoS One. 2017;12:e0172921.

4. Parisinos CA, Wilman HR, Thomas EL, Kelly M, Nicholls RC, McGonigle J, et al. Genome-wide and Mendelian randomisation studies of liver MRI yield insights into the pathogenesis of steatohepatitis. J Hepatol. 2020;73:241–51.

5. Andersson A, Kelly M, Imajo K, Nakajima A, Fallowfield JA, Hirschfield G, et al. Clinical Utility of Magnetic Resonance Imaging Biomarkers for Identifying Nonalcoholic Steatohepatitis Patients at High Risk of Progression: A Multicenter Pooled Data and Meta-Analysis. Clinical Gastroenterology and Hepatology. 2021.

6. Park CC, Nguyen P, Hernandez C, Bettencourt R, Ramirez K, Fortney L, et al. Magnetic Resonance Elastography vs Transient Elastography in Detection of Fibrosis and Noninvasive Measurement of Steatosis in Patients With Biopsy-Proven Nonalcoholic Fatty Liver Disease. Gastroenterology. 2017;152:598–607.e2.

7. Singh S, Allen AM, Wang Z, Prokop LJ, Murad MH, Loomba R. Fibrosis Progression in Nonalcoholic Fatty Liver vs Nonalcoholic Steatohepatitis: A Systematic Review and Meta-

555 analysis of Paired-Biopsy Studies. Clinical Gastroenterology and Hepatology. 2015;13:643–
556 54.e9.

557 8. Asaturyan H, Thomas EL, Bell JD, Villarini B. A Framework for Automatic Morphological
558 Feature Extraction and Analysis of Abdominal Organs in MRI Volumes. J Med Syst.
559 2019;43:334.

560 9. Liu Y, Basty N, Whitcher B, Bell JD, Sorokin EP, van Bruggen N, et al. Genetic
561 architecture of 11 organ traits derived from abdominal MRI using deep learning. Elife.
562 2021;10.

563 10. Penny WD, Friston KJ, Ashburner JT, Kiebel SJ, Nichols TE. Statistical Parametric
564 Mapping: The Analysis of Functional Brain Images. Elsevier; 2011.

565 11. Ramezani M, Johnsrude I, Rasoulian A, Bosma R, Tong R, Hollenstein T, et al.
566 Temporal-lobe morphology differs between healthy adolescents and those with early-onset
567 of depression. NeuroImage: Clinical. 2014;6:145–55.

568 12. Nakao M, Nakamura M, Mizowaki T, Matsuda T. Statistical deformation reconstruction
569 using multi-organ shape features for pancreatic cancer localization. Med Image Anal.
570 2021;67:101829.

571 13. Hori M, Okada T, Higashiura K, Sato Y, Chen Y-W, Kim T, et al. Quantitative Imaging.
572 Academic Radiology. 2015;22:303–9.

573 14. Biffi C, de Marvao A, Attard MI, Dawes TJW, Whiffin N, Bai W, et al. Three-dimensional
574 cardiovascular imaging-genetics: a mass univariate framework. Bioinformatics. 2018;34:97–
575 103.

576 15. Jia S, Nivet H, Harrison J, Pennec X, Camaioni C, Jaïs P, et al. Left atrial shape is
577 independent predictor of arrhythmia recurrence after catheter ablation for atrial fibrillation: A
578 shape statistics study. Heart Rhythm O2. 2021;2 6Part A:622–32.

579 16. Marvao A de, de Marvao A, McGurk KA, Zheng SL, Thanaj M, Bai W, et al. Phenotypic
580 Expression and Outcomes in Individuals With Rare Genetic Variants of Hypertrophic
581 Cardiomyopathy. Journal of the American College of Cardiology. 2021;78:1097–110.

582 17. Smith SM, Elliott LT, Alfaro-Almagro F, McCarthy P, Nichols TE, Douaud G, et al. Brain
583 aging comprises many modes of structural and functional change with distinct genetic and
584 biophysical associations. Elife. 2020;9.

585 18. Wang X, Vrtiska TJ, Avula RT, Walters LR, Chakkera HA, Kremers WK, et al. Age,
586 kidney function, and risk factors associate differently with cortical and medullary volumes of
587 the kidney. Kidney Int. 2014;85:677–85.

588 19. Fitzpatrick JA, Kim JU, Cobbold JFL, McPhail MJW, Crossey MME, Bak-Bol AA, et al.
589 Changes in Liver Volume in Patients with Chronic Hepatitis C Undergoing Antiviral Therapy.
590 J Clin Exp Hepatol. 2016;6:15–20.

591 20. Sudlow C, Gallacher J, Allen N, Beral V, Burton P, Danesh J, et al. UK biobank: an open
592 access resource for identifying the causes of a wide range of complex diseases of middle
593 and old age. PLoS Med. 2015;12:e1001779.

594 21. Littlejohns TJ, Holliday J, Gibson LM, Garratt S, Oesingmann N, Alfaro-Almagro F, et al.
595 The UK Biobank imaging enhancement of 100,000 participants: rationale, data collection,
596 management and future directions. Nature Communications. 2020;11.

597 22. Bayard M, Holt J, Boroughs E. Nonalcoholic fatty liver disease. Am Fam Physician.
598 2006;73:1961–8.

599 23. Sattar N, Forrest E, Preiss D. Non-alcoholic fatty liver disease. BMJ. 2014;349:g4596.

600 24. Sterling RK, Lissen E, Clumeck N, Sola R, Correa MC, Montaner J, et al. Development
601 of a simple noninvasive index to predict significant fibrosis in patients with HIV/HCV
602 coinfection. Hepatology. 2006;43:1317–25.

603 25. Yang G, Zhou S, Bozek J, Dong H-M, Han M, Zuo X-N, et al. Sample sizes and
604 population differences in brain template construction. Neuroimage. 2020;206:116318.

605 26. Whitcher B, Thanaj M, Cule M, Liu Y, Basty N, Sorokin EP, et al. Precision MRI
606 phenotyping enables detection of small changes in body composition for longitudinal
607 cohorts. Sci Rep. 2022;12:3748.

608 27. Thanaj M, Basty N, Liu Y, Cule M, Sorokin EP, Louise Thomas E, et al. Mass Univariate
609 Regression Analysis for Three-Dimensional Liver Image-Derived Phenotypes. Medical
610 Image Understanding and Analysis. 2021;:165–76.

611 28. Bai W, Shi W, de Marvao A, Dawes TJW, O'Regan DP, Cook SA, et al. A bi-ventricular
612 cardiac atlas built from 1000 high resolution MR images of healthy subjects and an analysis
613 of shape and motion. Medical Image Analysis. 2015;26:133–45.

614 29. Duan J, Bello G, Schlemper J, Bai W, Dawes TJW, Biffi C, et al. Automatic 3D Bi-
615 Ventricular Segmentation of Cardiac Images by a Shape-Refined Multi- Task Deep Learning
616 Approach. IEEE Trans Med Imaging. 2019;38:2151–64.

617 30. Smith S, Nichols T. Threshold-free cluster enhancement: Addressing problems of
618 smoothing, threshold dependence and localisation in cluster inference. NeuroImage.
619 2009;44:83–98.

620 31. Biffi et al. 2017. Biffi C. An introduction to mass univariate analysis of three-dimensional
621 phenotypes, https://github.com/UK-Digital-Heart-Project/mutools3D, R package version 1.0
622 (2017).

623 32. Benjamini Y, Hochberg Y. Controlling the False Discovery Rate: A Practical and
624 Powerful Approach to Multiple Testing. Journal of the Royal Statistical Society: Series B
625 (Methodological). 1995;57:289–300.

626 33. DeLand FH, North WA. Relationship between liver size and body size. Radiology.

627 1968;91:1195–8.

628 34. Heymsfield SB, Olafson RP, Kutner MH, Nixon DW. A radiographic method of
629 quantifying protein-calorie undernutrition. The American Journal of Clinical Nutrition.
630 1979;32:693–702.

631 35. Wynne HA, Cope LH, Mutch E, Rawlins MD, Woodhouse KW, James OF. The effect of
632 age upon liver volume and apparent liver blood flow in healthy man. Hepatology.
633 1989;9:297–301.

634 36. Johnson TN, Tucker GT, Tanner MS, Rostami-Hodjegan A. Changes in liver volume
635 from birth to adulthood: a meta-analysis. Liver Transpl. 2005;11:1481–93.

636 37. Yanaga K, Honda H, Ikeda Y, Nishizaki AT, Yamamoto K, Sugimachi K. Significance of
637 Liver Size in Hepatic Surgery. HPB Surgery. 1997;10:195–200.

638 38. Kratzer W, Fritz V, Mason RA, Haenle MM, Kaechele V, Roemerstein Study Group.
639 Factors Affecting Liver Size. Journal of Ultrasound in Medicine. 2003;22:1155–61.

640 39. Patzak M, Porzner M, Oeztuerk S, Mason RA, Wilhelm M, Graeter T, et al. Assessment
641 of liver size by ultrasonography. J Clin Ultrasound. 2014;42:399–404.

642 40. Kromrey ML, Ittermann T, vWahsen C, Plodeck V, Seppelt D, Hoffmann RT, et al.
643 Reference values of liver volume in Caucasian population and factors influencing liver size.
644 Eur J Radiol. 2018;106:32–7.

645 41. Marchesini G, Bua V, Brunori A, Bianchi G, Pisi P, Fabbri A, et al. Galactose elimination
646 capacity and liver volume in aging man. Hepatology. 1988;8:1079–83.

647 42. Younossi ZM, Golabi P, de Avila L, Paik JM, Srishord M, Fukui N, et al. The global
648 epidemiology of NAFLD and NASH in patients with type 2 diabetes: A systematic review and
649 meta-analysis. J Hepatol. 2019;71:793–801.

650 43. Younossi ZM, Blissett D, Blissett R, Henry L, Stepanova M, Younossi Y, et al. The
651 economic and clinical burden of nonalcoholic fatty liver disease in the United States and
652 Europe. Hepatology. 2016;64:1577–86.

653 44. Soufi M, Otake Y, Hori M, Moriguchi K, Imai Y, Sawai Y, et al. Liver shape analysis using
654 partial least squares regression-based statistical shape model: application for understanding
655 and staging of liver fibrosis. Int J Comput Assist Radiol Surg. 2019;14:2083–93.

656 45. Harbin WP, Robert NJ, Ferrucci JT Jr. Diagnosis of cirrhosis based on regional changes
657 in hepatic morphology: a radiological and pathological analysis. Radiology. 1980;135:273–
658 83.

659 46. Cunningham RP, Porat-Shliom N. Liver Zonation – Revisiting Old Questions With New
660 Technologies. Frontiers in Physiology. 2021;12.